

A NEW APPROACH TO CLAMPING IN MICRO WELDING

M204

Andreas Patschger¹, Andreas Hopf¹, Tobias Loose², Jens Bliedtner¹, Jean Pierre Bergmann³

¹ Ernst Abbe University of Applied Sciences Jena, Carl-Zeiss-Promenade 2, 07745 Jena, Germany

² Ingenieurbüro Tobias Loose (engineering office), Herdweg 13, 75045 Wössingen, Germany

³ Ilmenau University of Technology, Neuhaus 1, 98693 Ilmenau, Germany

Abstract

For the purpose of manufacturing lithium ion cells, micro welding is a commonly used procedure. It is also applied to new products as vacuum insulation elements which are enclosed in stainless steel foils. Another new application can be found in welding of catalytic converters. Before, they were usually joined by furnace brazing. All these products consist of thin metal foils which can be considered two-dimensional work pieces. They have to be joined in a stable process in order to avoid rejects. One of the biggest challenges in thermal micro welding is the gap forming between the joint partners due to thermally induced distortion. In micro welding, the possibility to bridge the gap between the joint partners is ensured as long as the gap is smaller than approximately half of the material thickness. Beyond this point, weld seam imperfections occur and the process collapses. In order to minimize gap formation, a new approach to clamping is presented which directly applies the clamping force in the welding zone. Based on this invention, a clamping fixture was constructed and qualified. Thereby, it is possible to close the gap between joint partners and adapt the properties of lap joints to bead-on-plate welds. Furthermore, the new concept was compared to a common clamping fixture. Thus, weldable joint partner thickness could be reduced, and the feeding rate was extended.

Motivation

Micro welding is defined by the dimensions of the joint partners. At least one dimension has to be smaller than $100\ \mu\text{m}$ [1]. This minimum requirement applies to thin metal foils, for example. The reason for this lies in the occurrence of scaling effects [2], [3]. Surface effects such as interfacial tension and, thus, the adhesive forces between fused material and base material, dominating volume effects such as the gravitational force [4]. In addition, thermally induced distortion grows exponentially to decreasing material thickness and scaled energy input per unit length [5]. This

change in effect dominance distinguishes micro welding from macro welding. On the one hand, aspect ratios of less than 0.2 are possible without backing and filler material (see Fig. 1(a)), but on the other hand, the thermally induced distortion causes the formation of gaps with material thicknesses of less than $100\ \mu\text{m}$ which can result in a process interruption due to bonding defects or holes in the weld seam [6]. The least the gap formation does, is to cause a seam collapse resulting in the reduction of seam and/or joint cross-section and, thus, a reduction in tensile strength (see Fig. 1 (b) - (d)).

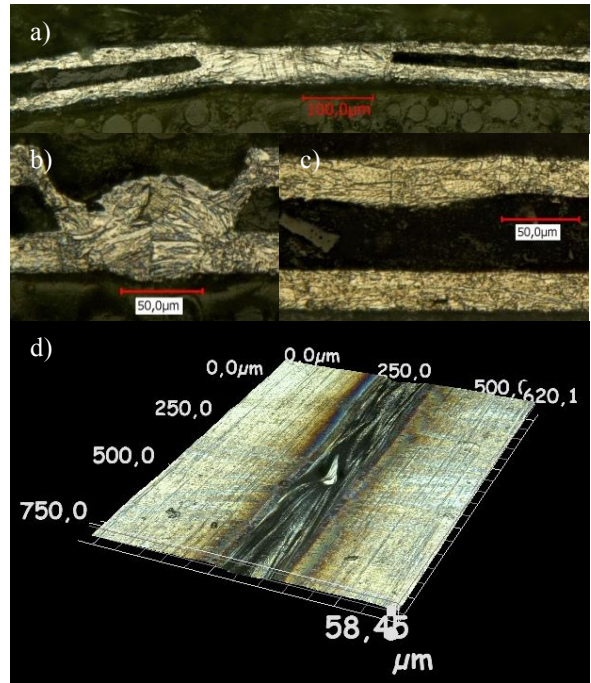


Figure 1: Welded metal foils; a) aspect ratio of 0.177; b) weld imperfection due to gap formation: seam collapse and reduction of the joint cross-section; c) bonding defect; d) hole formation

Hence, process reliability is jeopardized particularly in micro seam welding. Micro seam welding of thin steel foils is done wherever impermeability to gas or an enhanced joint stability is required [7]. In contrast to

spot welding, the beam energy is introduced through a weld path during micro seam welding. This raises the thermal load on the join partner and the tendency to warp at the same time. Micro joining is applied with steel foils for vacuum insulation panels (VIPs) [8], foil heat exchangers, catalysts [9], lithium ion batteries [10] and pressure sensors [11].

In order to be able to reliably weld seams in these products with foil thicknesses of $< 100 \mu\text{m}$, efficient processes and technologies are needed [12], [13], [14]. When it comes to welding seams in such dimensions, laser beam remote welding processes are particularly suitable [8], [15]. Thanks to their high energy density and, thus, the feasibility of high process speeds, thermal efficiency can be maximized [16].

However, laser beam welding is a thermal process causing energy to diffuse into the component by way of heat conduction. Despite the small amount of heat introduction, distortion of the join partners is inevitable [17]. Hence, not only the process itself needs to be designed efficiently, but the clamping fixture technology must be adapted as well. This is due to the low bending strength of the metal foils and to the development of residual welding stresses caused by the high temperature gradient. The latter is due to the fact that the process involves highly local action. When it comes to counteracting distortion and the associated gap formation, the clamping fixture plays a decisive role in the laser-based micro welding process.

To create a homogenous, continuous and impervious weld seam with material thicknesses of less than $100 \mu\text{m}$, realizing a technical zero gap between the join partners is the basic requirement [14], [18]. In the thermally dominated micro welding process, this is the requirement in terms of the clamping fixture that is independent of the process parameters.

State of the art

The welding process causes expansion and shrinkage effects in the component which are restrained by various influencing factors. In dependence on the site of action, a distinction can be made between local and global restraint to shrinkage. The local restraint to shrinkage is caused by colder material areas bordering on the heated weld seam. They restrain the expansion and shrinkage of the heated zones. This results in elastic-plastic deformations leading to component distortion and residual welding stresses after cooling. External clamping of the component or bracing by means of additional constructional elements causes stresses as a consequence of the global restraint to shrinkage. [19] That means that only the global restraint to shrinkage can be influenced by the

clamping fixture. The local restraint to shrinkage has to be controlled through an optimized welding process [20].

The clamping fixture can have an impact on the global restraint to shrinkage particularly via the restraint intensity and/or clamping length [21]. According to [22], these are defined as follows:

$$R_{Fy} = \frac{E \cdot h}{l_E} \quad (1)$$

R_{Fy} – restraint intensity; E – modulus of elasticity; h – foil thickness; l_E – clamping length

As the clamping length is reduced, the mean residual welding stresses grow transversely to the seam [23], while distortion decreases proportionally [20]. Moreover, the restraint intensity is an indicator of the probability of cold crack formation [24]. If the join connection is strained in the direction of the residual welding stresses, loading case and residual stresses will interfere with each other, and the mechanical strength of the joint will decrease. In case of unimpeded deformation (distortion), on the other hand, less residual stresses will develop in the work piece [25]. Thus, minimizing distortion and residual stress at the same time constitutes a classical conflict of objectives in fixture construction [23].

This conflict of objectives can only be solved by maximizing the clamping length and, thus, minimizing the residual stresses on the one hand, and by applying the clamping force in the joining zone of the lap joint to suppress distortion in the weld path on the other.

Various methods for the application of the clamping force in the joining zone have been described in the relevant literature:

According to [26], continuous contact between the join partners was achieved by integrating a cylindrical support on the bottom side of the weld path. In this way, the join partners with a thickness of $50 \mu\text{m}$ can be prestressed via the projecting weld and pressed against each other on a punctiform basis.

Another method was applied in [12] and [27] where a holding-down device in the form of a transparent plate was used to weld a thin metal foil to a thick substrate.

The use of a gas jet to apply the clamping force in the joining zone and fix the join partners in a gap-free manner is described in [28]. In this method, nozzles are positioned around the weld seam, and the foils are clamped hydrodynamically.

Within the scope of a research project [29], the mentioned clamping concepts were tested and qualified for metal foils with a thickness of less than 100 μm . Seam welding by means of modern laser beam sources of higher brilliance turned out to be not very practical. Consequently, a new clamping concept needs to be developed where the clamping force is applied within the joining zone, and the requirement of practicability is fulfilled as well.

Approach

In the case of the target application involving thin metal foils, the approach to a novel clamping concept is based on the controlled deformation of the upper join partner by applying a compressive force F_D (see Fig. 2). This can be realized easily due to the low flexural stiffness of the metal foils. That deformation increases the component stiffness considerably. The resistance to deformation perpendicular to foil surface is much higher in the peak of the deformation contour than it is the case with a flat, unformed foil. The resulting effect is that the compressive stresses developing in the course of welding do not cause any buckling.

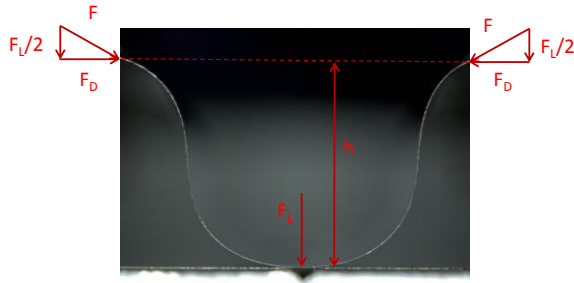


Figure 2: Schematic view of controlled deformation with force application

The vertical deformation h increases as the general deformation grows. As a result, the centric point load increases as well. With the help of the centric point load, a force F_L is generated which acts against the thermally induced distortion force during laser beam welding. The upper join partner is pressed against the bottom join partner such that a linear contact and/or small surface contact takes place and the point load acts upon the joining zone of the seam to be welded. The bottom join partner can additionally be fixed by means of a vacuum table.

Furthermore, the point load (generated force F_L) makes sure that the two join partners lie on top of each other without any gap in between, and that an optimized heat

transfer between the join partners is achieved. This approach has been patented [30].

Test arrangement

Laser sources, scanning units and beam properties

In order to be able to test the developed fixture concept under realistic industrial conditions, various modern solid state lasers suitable for micro seam welding were applied [3], [31], [32].

Table 1: Laser sources, scanning units and beam properties

| Laser | NovaDisc-P5 | FL X50 | 500W CW-M R4 "RS" |
|--|--------------|---------------|-------------------|
| Type | Disk laser | Fiber laser | Fiber laser |
| Manufacturer | Preno-vatec | Rofin-Sinar | SPI |
| Wavelength [nm] | 1,030 | 1,070 | 1,070 |
| Max. power [W] | 45 | 500 | 500 |
| Operating mode | cw | cw | cw |
| Optical fiber core / mode field diameter [μm] | - | 100 MM | 18.5 SM |
| Beam deflection unit | Superscan 20 | Turbo-scan 30 | Intelli-scan 20 |
| Manufacturer | Raylase | Raylase | Scanlab |
| Focal length collimation [mm] | - | 100 | 130 |
| Focal length F-Theta [mm] | 160 | 135/163 | 163/420 |
| Focal diameter* [μm] | 25 | 144/164 | 25/ 65 |
| Beam quality* | 1.2 | 8.6 | 1.1 |

* Measured @ 10 % of the max. power

Test specimens

Cold-rolled 1.4301/AISI304 stainless steel foils in thicknesses of 5 μm up to 100 μm were used for the studies. The foils were cut into coupons, clamped and welded in the form of a lap joint.

Reference fixture

In order to be able to compare the new fixture concept, a customary clamping fixture was chosen where the clamping force is applied along the weld path. The clamping length (distance of the upper clamping strips) is 8 mm, while the groove width measures 5.5 mm.

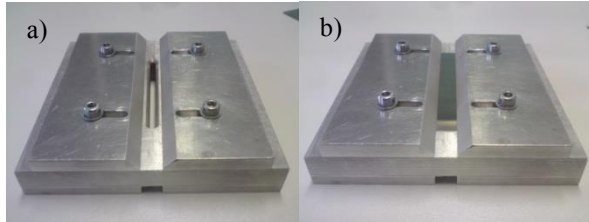


Figure 3: a) Clamping fixture only; b) with fixed foils in a lap joint

Simulation of the reference fixture properties

In order to qualify the distortion and the residual stresses in the metal foils during and after the micro welding process and to compare them later on, a weld pattern simulation was carried through. For this purpose, two 50 μm foils were welded together in the form of a lap joint on the reference fixture using the NovaDisk P5. The laser power and feeding rate process parameters were 17 W and 7.5 mm/s at a focal diameter of 25 μm .

Heat introduction is not simulated, but predefined as an input parameter and realized by means of a substitute heat source. The latter is designed such that the same heat introduction as in the experiments is achieved. The other boundary conditions of the weld pattern simulation can be found in [20].

The shrinkage of the material during the cooling phase causes high tensile stresses in the longitudinal direction of the weld seam. That shrinkage is restrained by the surrounding colder component areas (locally) and by the clamping situation (globally). The residual stresses acting transversely to the seam are comparatively small due to the small restraint intensity. As the equilibrium of forces must be maintained, the longitudinal tensile stresses cause compressive stresses in the base material. [23]

Compressive stresses caused by shrinkage can lead to instability with thin components. Distortion in the form of buckling is the result, entailing major deformations developing perpendicularly to the foil plane. Superimposed angular shrinkage can even intensify this effect [23].

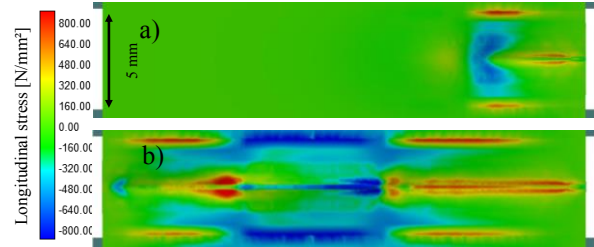


Figure 4: Simulated longitudinal stress on the upper side of the upper foil a) at the beginning of the welding process and b) after welding (tensile stresses - red; compressive stresses - blue)

Figure 4 shows the simulated longitudinal stress at the beginning and after the welding process. During the welding process a compressive stress bulb section forms in front of the heat source. The diffusion of the compressive stress constitutes the main cause of the buckling observed. The residual stress pattern shown in Fig. 4 (b) is the result of the interference of distortion stresses and residual welding stresses.

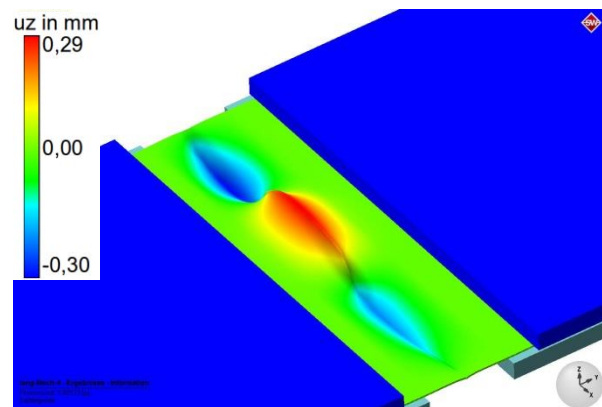


Figure 5: Simulated vertical distortion after welding in overlap joint (image exaggerated by a factor of 5)

Figure 5 shows the vertical distortion in the form of buckling over a simulated weld seam length of 24 mm. The simulated buckling causes a significant risk of gap formation between both join partners as the amplitude of the simulated distortion of the upper foil reaches 0.3 mm. Assuming a non-buckling surface of the lower foil or even a negative amplitude of distortion in the same order, a gap in magnitude of a single foil thickness would occur. Therefore, buckling of the foils must be prevented in order to design a reliable process.

The shape of the simulated buckling was also observed with the real coupons welded on the reference fixture (see Fig. 6).

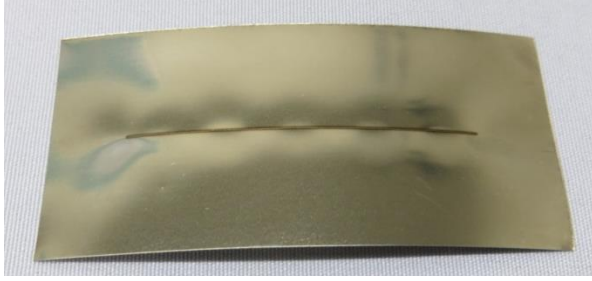


Figure 6: Buckling in a welded test coupon (2 x 50 μm) with a weld path length of 30 mm

Qualification of the new fixture concept

Setup and performance testing of a test fixture

The developed clamping concept was implemented using a test fixture.

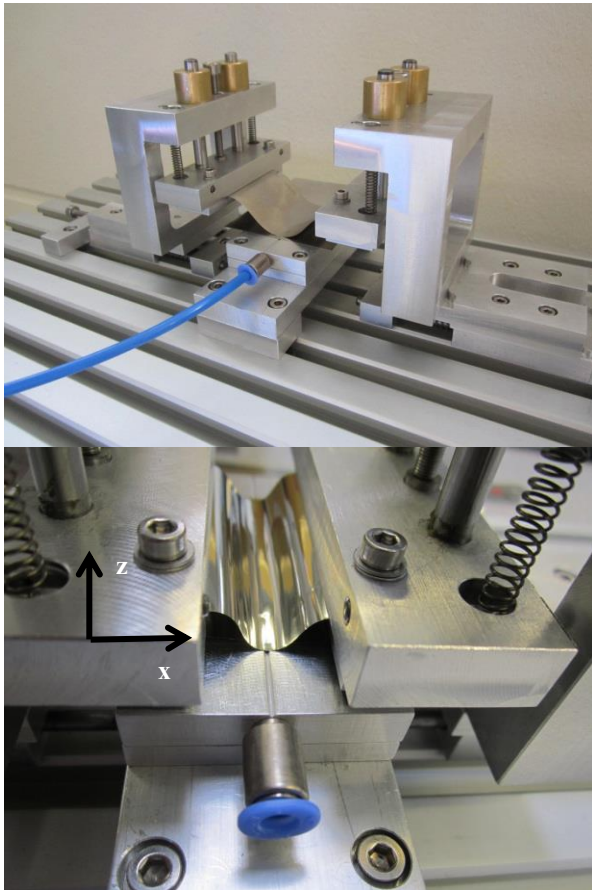


Figure 7: Test fixture for clamping concept testing

The upper join partner is placed in a holding fixture, and the bottom join partner is positioned on the base plate. To ensure stable fixation, a vacuum table is used which has a groove so that the welding process is not impeded. The adjusting unit moves the holding fixtures

towards each other in the x-direction. Due to the movement of the adjusting unit in the x-direction, the upper join partner is deformed. While it is in this deformed position, it is moved in the z-direction by means of a second adjusting unit. In this way, the foils to be joined are pressed against each other. As soon as the two join partners have formed a common contact surface, the actual joining process can begin.



Figure 8: Welded test coupon (2 x 50 μm) with a weld path length of 30 mm without buckling

Fig. 8 shows a welded test coupon produced using the test fixture. Thanks to the increased stiffness of the systematically deformed upper foil, buckling due to the compressive stresses applied during the welding process is avoided. The difference between Figure 6 and Figure 8 is clearly visible.

Clamping force determination

The pressing force F_L of the test fixture for various foil thicknesses was measured using a force sensor (HBM load cell of the type U1R).

Table 2: Achievable pressing force for different foil thicknesses

| Foil thickness in μm | Force in N |
|----------------------|------------|
| 50 | 4 |
| 25 | 2 |
| 15 | 0.15 |

Impact of the groove width on process efficiency

In [33] the effect of the clamping elements as a heat sink is described for the laser beam welding of thin metal foils. The greater the distance of the clamping elements from the joining zone, the smaller the heat loss, and the more process energy is available. This manifests itself in a greater seam volume and/or in a larger seam cross-sectional area.

In order to examine the impact of the heat sink effect in the new clamping concept, the weld seam cross-sectional area can be used as an indicator. When the energy input per unit length remains constant, the weld seam cross-sectional area is proportional to the process efficiency [34], i.e. the higher the heat loss, the lower

the process efficiency and the smaller the weld seam cross-sectional area.

Vacuum tables with different groove widths were built for this examination and tested by welding two 50 μm foils together in the form of a lap joint to compare the results. In this context, welding was performed on the basis of both the deep welding regime and the heat conduction welding regime. All tests were repeated five times. Then the mean value of the seam areas was calculated and examined in the following diagram in dependence on the groove width.

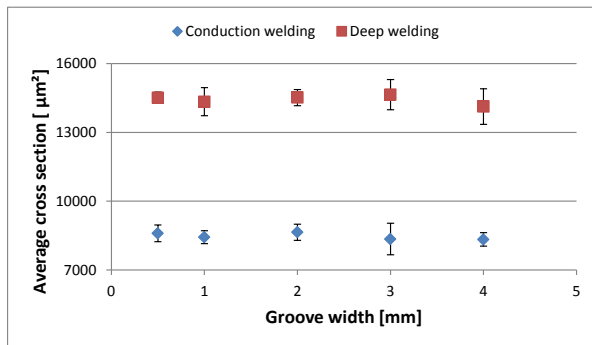


Figure 9: Average seam cross-sectional areas with standard deviation in dependence on the groove width for a heat conduction welding process ($v = 80 \text{ mm/s}$ @ $P = 50 \text{ W}$) and a deep welding process ($v = 825 \text{ mm/s}$ @ $P = 400 \text{ W}$), welded using the FLX50 ($d_f = 164 \mu\text{m}$)

A statistical regression analysis of the mean values resulted in a p -value of 0.216 (heat conduction welding) and 0.545 (deep welding). The p -value is the probability of obtaining a test statistic result at least as extreme or as close to the one that was actually observed, assuming that the null hypothesis is true. Regarding a significance level of 0.05, the null hypothesis cannot be rejected, and there is no significant correlation between seam cross-sectional area and groove width. That means that welding with the new fixture concept is possible at constant process efficiency independently of the groove width.

Comparative examination of the fixtures

Formation of the joint gap along the micro weld seam

The size of the joint gap is the actual target criterion of the new fixture concept. In a first step, the formation of the joint gap along the weld seam is to be examined for both the test fixture and the reference fixture. For that purpose, each two 50 μm thick steel foils were welded together in a lap joint on both fixtures using an FLX50 laser ($d_f = 164 \mu\text{m}$) with a power of 300 W and at a feeding rate of 550 mm/s. The welded test coupons

were segmented and prepared, and then the gap was measured.

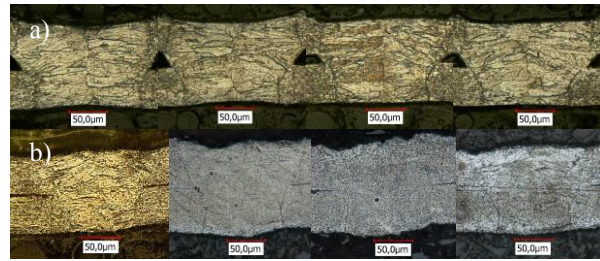


Figure 10: Gap formation along the weld seam a) with the reference fixture and b) with the test fixture (new clamping concept), starting 2 mm after the beginning of the seam and occurring with a spacing of 10 mm

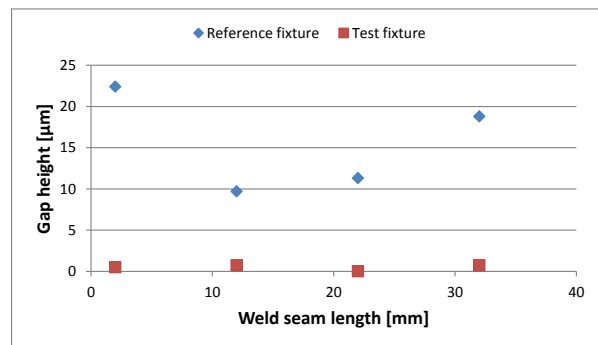


Figure 11: Measured gap heights along the weld seam for both fixtures

Figures 10 and 11 show the unsteady gap height with the reference fixture, while the test fixture exhibits a constant technical zero gap. Thus, the new clamping concept provides technically ideal thermal coupling of the two joint partners.

Comparison of lap welds to bead-on-plate welds

To examine thermal coupling and unimpeded heat transfer, welding tests were performed applying defined process parameters to bead-on-plate welds and lap welds on both fixtures. The weld seam cross-sectional areas obtained at constant energy inputs per unit length were compared and evaluated. In this procedure, the CW-M R4 “RS” laser with focal diameters of 25 μm and 65 μm was used. The energy inputs per unit length were selected in dependence on focal diameter and power such that full penetration welding of the each two 50 μm and two 25 μm foils was just about feasible.

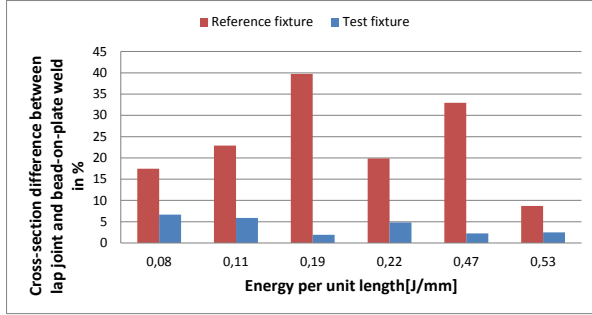


Figure 12: Percentage difference between weld seam cross-sectional areas of lap joints (2 x 50 μm) and bead-on-plate welds with a 100 μm foil, welded on the reference fixture and on the test fixture (new clamping concept)

Figure 12 shows that the weld seam cross-sectional area severely varies along with the varying joint gap of the reference fixture. The percentage difference compared to the bead-on-plate weld grows as high as 40 %. The test fixture with the new clamping concept, in contrast, is capable of constantly keeping the seam cross-sectional area below 10 % at constant energy inputs per unit length. The remaining offset is attributable to the enlarged surface of the bent foils (see Fig. 7) which causes a greater cooling effect due to convection. Hence, the test fixture achieves a technically ideal heat transfer between the joint partners, comparable to the solid material.

Achievable maximum speed at defined weld seam depth

According to [35], the achievable maximum process speed v_{max} correlates with the quotient of absorbed power P and welding depth s as well as focal diameter d_f , the so-called drawn power.

$$v_{max} \propto \frac{P}{s \cdot d_f} \quad (2)$$

The drawn power serves as a reference plot. The higher v_{max} at a constant drawn power, the higher the process efficiency.

Applying a focal diameter of 25 μm, welding tests were performed using the NovaDisc-P5 with both fixtures and at a constant drawn power. Since welding depth and focal diameter were kept at constant levels with each foil thickness, the power has been plotted over the feeding rate in the following figure for the sake of clarity. Blue data points represent the reference fixture, while red data points stand for the test fixture with the new clamping concept.

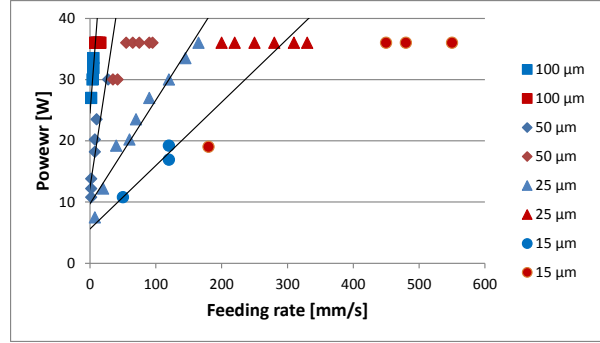


Figure 13: Power in dependence on the speed for both fixtures and various foil thicknesses (The trend lines relate to the data sets of the reference fixture – blue.)

In Figure 13 the data sets of equal foil thicknesses can be compared to each other as they were machined with the same focal diameter and also exhibit the same welding depth. That means that at a constant power level the process efficiency grows as the maximum speed increases. Since at equal welding depth, power and focal diameter the maximum speed is higher with the test fixture than with the reference fixture, higher process efficiency can be achieved with the former compared to the reference fixture.

This also becomes apparent when the energy input per unit length is calculated:

$$E = \frac{P}{v} \quad (3)$$

The energy input per unit length is a measure of the heat load on the component [34], and it decreases when the speed grows and the power remains constant.

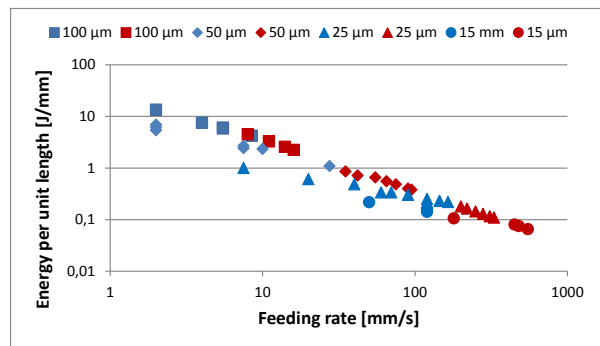


Figure 14: Double logarithmic representation of the energy input per unit length in dependence on the feeding rate for both clamping fixtures and various foil thicknesses

Figure 14 clearly shows that when welding the same foil thicknesses using the test fixture, the energy input per unit length and, thus, the heat load decreases.

Weldable minimum joint partner thickness

When the heat load due to the energy input per unit length declines with a constant foil thickness, distortion will decrease as well [5]. Hence, it is also possible to join metal foils with a focal diameter that is greater than the material thickness.

Especially when it comes to small focal diameters, the minimum thickness of the individual foil to be joined can be reduced (see Fig. 15). Greater focal diameters have the benefit of better gap bridgeability. Furthermore, physical limits are established by the aspect ratio in the weld pool. Consequently, the differences are marginal here.

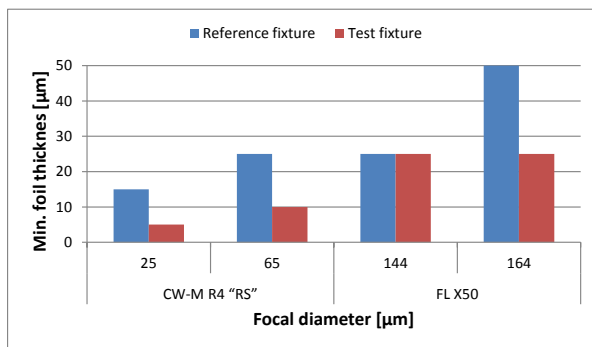


Figure 15: Minimum foil thickness to be joined in dependence on focal diameter and fixture type

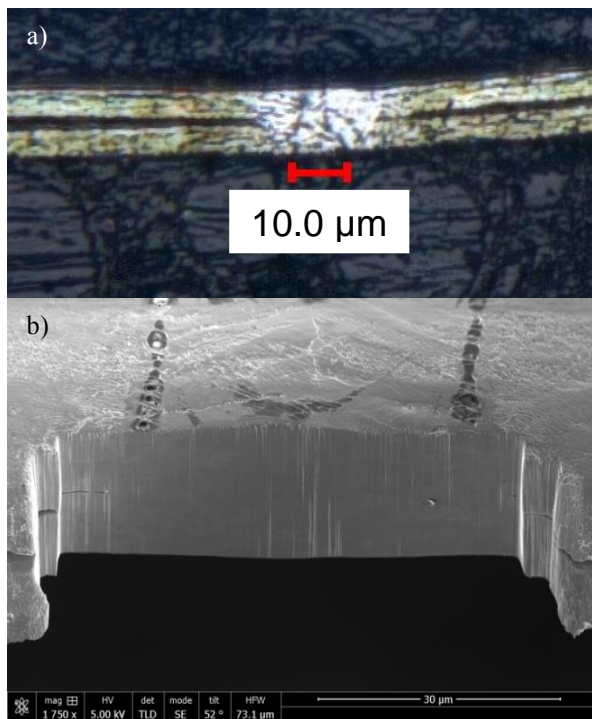


Figure 16: Cross-sections of micro welds with $d_f = 25 \mu\text{m}$; a) two $5 \mu\text{m}$ foils ($v = 2,500 \text{ mm/s}$ @ 25 W) and b) two welded $10 \mu\text{m}$ test coupons prepared by means of a focused ion beam

In Figure 16, the technical zero gap between the joint partners can be recognized very well. Test coupons with a very small material thickness can thus be joined without any problems.

Tolerated joint gap height

Limited joint gaps are required for reproducible lap joints in welding practice. The maximum gap heights, for example, may measure 5 - 10 % of the individual sheet thickness and/or $150 \mu\text{m}$ altogether at the highest [36]. For the following examinations the NovaDisk P5 and the FL X50 laser were applied with focal diameters of $25 \mu\text{m}$, $144 \mu\text{m}$ and $164 \mu\text{m}$. The thicknesses of the foils welded together in the form of a lap joint were $15 \mu\text{m}$, $25 \mu\text{m}$, $50 \mu\text{m}$ and $100 \mu\text{m}$. About 70 welding tests were performed on the two welding fixtures, and then the joint gaps were measured. On that basis, the percentage joint gap was classified in relation to the foil thickness for both fixtures.

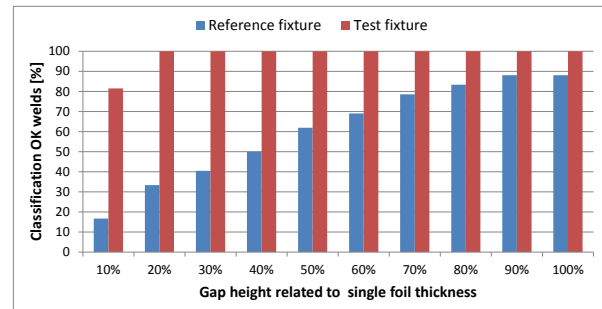


Figure 17: Joint gap classification in relation to the foil thickness and the resulting classification as OK welds

When applying the quality criterion from [36], 81 % of the welds (10 % class) produced on the test fixture can be considered OK welds, whereas only 17 % OK welds can be achieved using the reference fixture (see Fig. 17). The 20 % gap height class related to the individual foil thickness already includes 100 % of all welds produced by means of the test fixture. That means that when using the test fixture, the gap does never exceed 20 % of the individual foil thickness in the examinations. In contrast, not even 90 % of the welds produced on the reference fixture exhibited a gap height equal to or smaller than the foil thickness.

Summary

In the present paper, a novel, patented clamping concept was introduced by means of which thin metal foils can be welded together efficiently and reliably by way of micro welding. Compared to an industry-standard clamping concept, the new fixture concept has achieved the following improvements:

- Minimization of the joint gap (less than 20 % of the foil thickness) and keeping it at a constant level
- Increase in process efficiency by raising the maximum process speed at a constant drawn power and lowering the energy input per unit length while the welding depth remains the same
- Achievement of a technically ideal heat transfer between the join partners
- Minimization of the weldable foil thicknesses down to 5 μm

Outlook

As a next step, welding distortion and residual compressive stress are to be simulated for the test fixture and theoretically compared to the reference fixture. During the further procedure, the fixture will be advanced for industrial application and adapted to the use with coils. Thus, the foils will no longer have to be cut prior to welding.

Acknowledgements

The authors are particularly grateful to the BMWi and the AIF for funding considerable parts of the work in the context of a ZIM project.

References

- [1] Zhou, Y. (2008) Microjoining and Nanojoining, Woodhead Publishing Ltd, Cambridge, England, 2008.
- [2] Vollertsen, F., Wagner, F., Thomy, C., (2007) Micro welding for environmental-friendly products, Proc. of ICALEO, 26th int. Cong. on Applications of Lasers and Electro-Optics, Orlando, USA, LIA Publication 610 (CD), 308, p. 143-148.
- [3] Patschger, A., Bliedtner, J., Bergmann, J.P. (2014) Process-limiting Factors and Characteristics of Laser-based Micro Welding, In: Proc. Of Laser Assisted Net shape Engineering, Physics Procedia, IN PRESS.
- [4] Wautelet, M. (2001) Scaling Laws in the Macro-, Micro- and Nanoworlds, Eur. J. Phys. 22, p. 601–611.
- [5] Thomy, C., Möller, F., Vollertsen, F. (2010) Distortion effects in micro welding with fibre laser, Proc. of ICALEO, 29th int. Cong. on Applications of Lasers and Electro-Optics, Anaheim, USA, LIA Publication 613 (CD), 301, p. 85-90.
- [6] Patschger, A., Bliedtner, J., Bergmann, J.P. (2013) Approaches to Increase Process Efficiency in Laser Micro Welding, Physics Procedia, volume 41, pages 585-595, ISSN 1875-3892.
- [7] Qin, Y. (Ed.), (2010) Micromanufacturing Engineering and Technology, Elsevier, Oxford, p. 196.
- [8] Patschger, A., Bergmann, J.P., Bliedtner, J. (2012) Flexible and Efficient Laser Remote Welding of Ultra-thin Metal Foils, J. Laser Appl. 24, 052005, 2012.
- [9] Patent DE2727967C2 The monolithic metal catalyst to detoxify the exhaust gases of internal combustion engines, especially in motor vehicles, as well as methods for the manufacture thereof.
- [10] Dürr, U., Holtz, R., Westphäling, T. (2006) Industrielle Anwendungslösungen mit gepulsten Nd:YAG Lasern (Industrial Application Solutions Involving Pulsed Nd:YAG Lasers). In: Strahltechnik (Beam Technology), volume 28: Tagungsband zum 5. Laser Anwenderforum (Conference Transcript of the 5th Laser User Forum), Bremen: BIAS-Verlag publishing house.
- [11] Hanebuth, H., Lupp, F. (2010) Abschlussbericht zum FuE-Vorhaben 13 N 8990 im Verbundprojekt “Schädigungsarmes und produktives Mikroschweißen mit brillanten Strahlquellen” - SCHARP, Teilvorhaben: “Grundlagen für Applikationen im Medizin- und Automobilbereich” (Final Report on the R&D Project 13N 8990 within the Scope of the Joint Research Project “Low-damage and Productive Micro Welding with Brilliant Laser Sources” - SCHARP, Subproject: “Basic Concepts of Applications in Medical and Automotive Sectors”). Munich: Siemens AG.
- [12] Abe, N., Funada, Y., Tsukamoto, M. (2008) Welding of Thin Foils with Elliptical Beams. Transaction of JWRI, Issue No. 1.
- [13] Löffler, N. (2012) Laseranwendungen mittels 532 nm in dem Bereich elektronischer Bauteile (Laser Applications with 532 nm in the Field of Electronic Components). In: Tagungsband (conference transcript): LEF 2012. Bamberg: Meisenbach.

- [14] P'ng, D., Molian, P. (2007) Q-switch Nd:YAG welding of AISI 304 stainless steel foils. *Materials Science and Engineering*, volume 486, pp. 680-685.
- [15] Kleemann, G. (2012) Voraussetzung für zuverlässige Verbindungen beim Laser-Mikroschweißen (Precondition for Solid Bonds in Laser Micro Welding). In: Tagungsband (conference transcript): LEF 2012. Bamberg: Meisenbach.
- [16] Dausinger, F. (1995) Strahlwerkzeug Laser: Energieeinkopplung und Prozeßeffektivität (The Laser as a Beam Tool: Energy Coupling and Process Efficiency), habilitation, University of Stuttgart, B.G. Teubner Verlag publishing house, Stuttgart, p.87.
- [17] Okamoto, Y. et al. (2007) Fine micro-welding of thin metal sheet by high speed laser scanning. In: Proc. of SPIE Vol. 6593, 65930D.
- [18] Ventrella, V. A., Berretta, J. R., de Rossi, W. (2010) Pulsed Nd:YAG laser seam welding of AISI 316L stainless steel thin foils. *J. Mater. Process. Tech.* Vol. 210, Nr.14, p. 1838-1843.
- [19] Kannengießler, T. (2000) Untersuchung zur Entstehung schweißbedingter Spannungen und Verformungen bei variablen Einspannbedingungen im Bauteilschweißversuch (Examination on the Development of Tensions and Deformations due to Welding under Variable Clamping Conditions in a Component Welding Test). Aachen: Shaker Verlag publishing house.
- [20] Loose, T., Patschger, A., Bliedtner, J. (2014) Simulation-aided Optimization of a Laser-based Micro-welding Process. In: *Thermal Forming and Welding Distortion, Strahltechnik (Beam Technology)* volume 54, BIAS Verlag publishing house, Bremen, p. 141-158.
- [21] Wohlfahrt, H., Dilger, K. (2004) Eigenspannungen in Schweißverbindungen - ihre Entstehung und Bewertung (Residual Stresses in Welded Joints and their Development and Assessment). TU Braunschweig: DVS seminar.
- [22] Satoh, K., Ueda, Y., Kihara, H. (1972) Recent Trend of Researches on Restraint Stresses and Strains for Weld Cracking. *Transactions of JWRI*, pp. 53-68.
- [23] Dilthey, U. (2005) Schweißtechnische Fertigungsverfahren 2: Verhalten der Werkstoffe beim Schweißen (Manufacturing Processes Based on Welding Engineering 2: Behavior of Materials during Welding). Heidelberg: Springer-Verlag GmbH Co. KG publishing house.
- [24] Lachmann, C., Nitschke-Pagel, T., Wohlfahrt, H., 1999. Zum Einfluß von Eigenspannungen und Mikrostruktur auf die Kaltrißneigung hochfester Stähle (On the Influence of Residual Stresses and Microstructure on the Cold Cracking Tendency of High-strength Steels). In: *Eigenspannungen und Verzug durch Wärmeeinwirkungen (Residual Stresses and Distortion due to Heat Exposure): Forschungsbericht (DFG Series research report)*. S.I.: John Wiley & Sons.
- [25] Radaj, D. (1988) Wärmeeinwirkungen des Schweißens - Temperaturfeld, Eigenspannungen, Verzug (Heat Exposure during Welding - Temperature Field, Residual Stresses, Distortion). Heidelberg: Springer-Verlag publishing house.
- [26] Brockmann, R. (2003) Beitrag zum Mikronahtschweißen von Edelstahlfolien mittels dioden-gepumptem Nd:YAG-Laser (Article on the Micro Welding of Stainless Steel Foils by Means of a Diode-pumped Nd:YAG Laser). Aachen: Shaker Verlag publishing house.
- [27] Lingenfelter, A. C. (1986) Laser welding of thin cross sections, CA (USA): Lawrence Livermore National Lab.
- [28] Osborne, R. F. (1976) Clamping of Film-Like Material for Radiant Energy Welding. USA, patent no. 3997385.
- [29] N.N. (2012) Zwischenbericht DüFoS - Effizientes und flexibles Remote-Schweißen von ultradünnen metallischen Folien (DüFoS Interim Report – Efficient and Flexible Remote Welding of Ultrathin Metal Foils), no. KF 2242302SU1.
- [30] Patent DE 10 2013 019 405
- [31] Patschger, A., Güpner, M., Bliedtner, J., Bergmann, J.P. (2013) Remote micro welding with multi-mode and single-mode fiber lasers – a comparison, 32nd int. Cong. on Applications of Lasers and Electro-Optics, Anaheim, USA, LIA Publication 616 (CD), M603, p. 805-815.
- [32] Strocka, S., Hopf, A., Patschger, A., Bliedtner, J., Hild, M., Störzner, F. (2012) Beitrag zur Prozessentwicklung für das Remote-Laser-Schweißen von dünnen metallischen Folien (Contribution to Process Development for Remote Laser Welding of Thin Metallic Foils), 22. Internationale Wissenschaftliche Konferenz Mittweida (22nd International Scientific Conference in Mittweida), Mittweida, Germany.

[33] Du, J., Longobardi, J., Latham, W.P., Kar, A. (2002) Laser marginal lap welding for ultrathin sheet metal, J. Laser Appl. 14, Nr. 1, February 2002, p. 4-8.

[34] Hügel, H., Graf, T. (2009) Laser in der Fertigung – Strahlquellen, Systeme, Fertigungsverfahren (Lasers in Manufacturing – Beam Sources, Systems, Manufacturing Processes), 2nd edition, GWV specialized publishers, Wiesbaden.

[35] Dausinger, F. (1995) Strahlwerkzeug Laser: Energieeinkopplung und Prozeßeffektivität (The Laser as a Beam Tool: Energy Coupling and Process Efficiency), habilitation, University of Stuttgart, B.G. Teubner Verlag publishing house, Stuttgart, p.87.

[36] Reek, A. (2000) Strategien zur Fokuspositionierung beim Laserstrahlschweißen (Strategies for Focus Positioning in Laser Beam Welding), Forschungsberichte iw b (iw b research reports), volume 138, Herbert-Utz-Verlag publishing house, and also: dissertation, Munich, Technische Universität München, 2000.

Meet the Author

Andreas Patschger received his diploma in mechanical engineering from the University of Applied Sciences in Jena, Germany, in 2004. In 2006, he earned the degree of a Master of Engineering in Laser and Optical Technologies at the same university.

From 2006 to 2010, he worked as a service engineer in the field of the commissioning and maintenance of laser material processing systems and, later on, as an application engineer at JENOPTIK AG, Germany.

Since 2010, he has been working as a scientific associate and now as head of the laser welding group at the department of production engineering of the Ernst Abbe University of Applied Sciences in Jena, Germany.